Photochemistry

DOI: 10.1002/ange.201304321

Multiple Photoluminescence from 1,2-Dinaphthyl-*ortho*-Carborane**

*Kyung-Ryang Wee, Yang-Jin Cho, Jae Kyu Song, and Sang Ook Kang**

A special feature of multiple photoluminescence in a single organic molecule is that it is only reported for geometrically unique systems. These molecules have drawn much attention because of their paradoxical photophysical behavior, contradicting Kasha's rule, which is a principle in the excited molecules.[1] The rule states that photoluminescence occurs in an appreciable yield only from the lowest excited state.[2] Multiple emissions arise from the corresponding nonequilibrated excited states, rather than from the most stable excited state. The existence of energetically feasible excited states comes from the restricted molecular conformation where organic functional groups occupy the most favorable geometrical positions at only small energy costs.[3] A few examples are available in which multiple photoluminescence are elaborated: adiabatic photoreactions such as excited-state proton transfer[4] (ESIPT), and excimer[5] and twisted intramolecular charge-transfer[6] (TICT) state formation (see each example in Scheme 1).

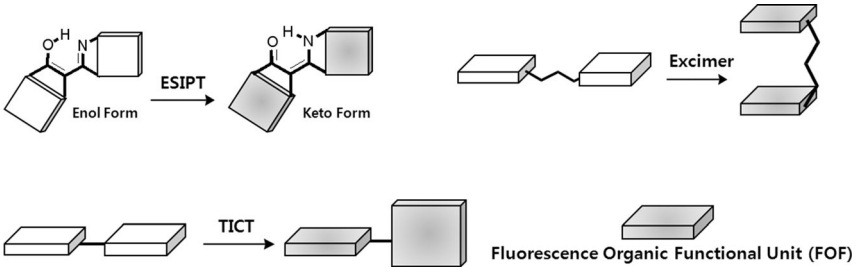

Scheme 1. The preponderances of multiple photoluminescence (ESIPT = excited-state proton transfer) and TICT = (twisted intramolecular charge transfer).

In line with observing multiple photoluminescence and understanding the working principle underlining the photoluminescence, we paid special attention to the molecular entity[7] which would even further support serial excited states. We noted recently that *ortho*-carborane facilitates the stabilization of an excited state that would otherwise be unable to be accommodated.[8] Such an excited-state stabilization could provide a new entry of multiple photoluminescence.[9] Indeed, when we brought two fluorescence organic functional (FOF) units into the *o*-carborane framework, unprecedented multiple photoluminescence developed. Scheme 2 shows the involvement of two FOFs on the surface

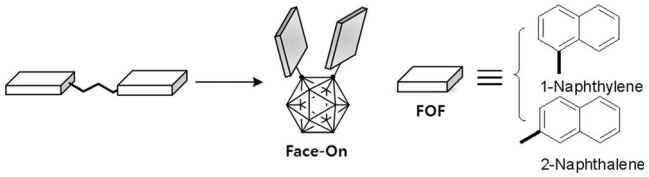

Scheme 2. Multiple photoluminescence using *ortho*-carborane.

of a *o*-carborane molecule, showing that a linear array of FOF is transformed to a "Face-On" conformation upon incorporation into the *o*-carborane cage. FOFs used herein involve two isomeric forms of naphthalene, 1- or 2-naphthyl, as shown in Scheme 2.

Naphthalene is one of the well-understood FOF groups.[10] By estimating the geometrical preference of the two naphtalene units within the *o*-carborane skeleton, we introduced naphthalenes to the carbon atoms of the *o*-carborane. Because of the three-dimensional bonding of *o*-carborane,[11] attachement to the two carbon atoms induces a specific orientation for the engaging naphthalenes. Later, we established an exact conformation created by the two naphtalene groups from X-ray structural studies to be in a "face-on" (see Scheme 2) conformation, and this constellation casts multiple photoluminescence.

As shown in Figure 1, with the variation of a 1- or 2-isomeric form of naphthalene, 1,2-dinaphthyl-o-carboranes (**1** and **2**) were prepared according to the acetylene incorporation protocol[12] (see synthetic details in the Supporting Information). One of the notable features found in each structure is that the carbon–carbon distances in the *o*-carborane cage are significantly elongated[13] and **1** has an even longer distance relative to **2**, indicating that **1** significantly induces cage deformation.

UV/Vis absorption spectra of **1** and **2** were measured in solution and compared with those of diphenyl-o-carborane (Ph-Cb). As shown in Figure S2 and Table S3, the absorption

[*] K.-R. Wee, Y.-J. Cho, Prof. S. O. Kang
Department of Advanced Materials Chemistry
Sejong-ro 2511 Korea University
Sejong-city 339-700 (South Korea)
E-mail: sangok@korea.ac.kr
Prof. J. K. Song
Department of Chemistry, Kyung Hee University
Seoul 130-701 (South Korea)

[**] This work is supported by the Korea Evaluation Institute of Industrial Technology (KEIT) funded by the Ministry of Knowledge Economy (MKE, Korea) through the Improving Competitiveness of Materials and Components Industry Program (grant number 10042682). We also acknowledge the Chungcheong Institute for Regional Program Evaluation (CIRPE, grant number A0046 00226).

Supporting information for this article is available on the WWW under http://dx.doi.org/10.1002/anie.201304321.

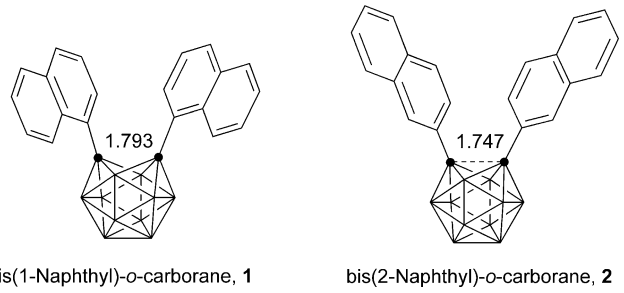

Figure 1. Structures of **1** and **2**. The numbers represent the carbon–carbon distances in Å.

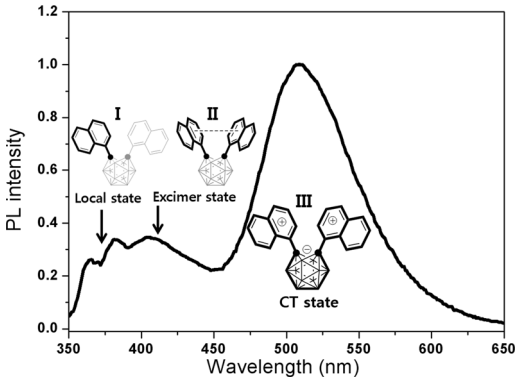

Figure 2. Multiple photoluminescence from **1** in hexane solution upon excitation at 325 nm.

spectra differ from the reference naphthalene[10] and are red-shifted within 25 nm for the ^1L_a and ^1L_b bands with less vibrational structures, commonly showing π–π* transitions originating from naphthalene.[10,14] A distinctive red-shift of the peaks at around 330–400 nm was observed for **1**. From the spectral comparison between **1** and **2** and Ph-Cb, **1** appears to have a unique ground state.

The emission spectra of **1** and **2** differ markedly from that of the naphthalene chromophore upon excitation at 325 nm,[14] showing multiple emissions between 350 and 450 nm and below 500 nm. A multiple emission feature is more pronounced for **1**; the first two disparate emissions were clearly seen at 381 and 420 nm and assigned for the ^1L_b state of the naphthalene chromophore and the excimer[15] between the two naphthalene groups facing each other, respectively. The second broad red-shifted emission of **1** at around 508 nm was assigned to a charge-transfer (CT) excited state, as shown by the remarkable solvatochromic shifts of the emission in Figure S3. Monomer and excimer emissions can be easily overlooked by the dominant CT emission.

To address the origin of multiple emissions, serial excitation spectra were taken for **1** at 360, 380, 420, and 508 nm (Figure 2). The excitation spectra of **1** differed significantly when monitored at 380 nm for the local emission or at 420 nm for the excimer emission, and at 508 nm for the CT emission. As shown in Figure S6, the excitation spectrum monitored at 508 nm approximately traces the absorption spectrum, particularly at <300 nm, whereas the monomer and excimer emissions give an excitation spectrum with a maximum at 350 nm, which substantially differs from the absorption spectrum. Accordingly, when naphthalene is covalently bonded to the 1,2-position of *o*-carborane, a distinctive CT emission appears with extensive quenching of the naphthalene fluorescence and the CT state is isolated from the high-energy local excited states of naphthalene.

The inset of Figure 3a shows emission decay profiles for **1** monitored at 380 nm, which are commonly fitted to single-exponential kinetics with lifetimes of 1.8–2.3 ns. Similarly, the lifetimes of excimer emissions (at 420 nm, Figure S7) in different solvents were determined as 1.9–2.8 ns. On the other hand, the CT emission monitored at 508 nm shows considerably shorter lifetimes (≤ 0.4 ns), as shown in Figure 3a. Therefore, we assumed that the low energy of the CT states is isolated from local excited states and shows an independent behavior, which is well matched with excitation spectra. In addition, the CT states show a strong dependence on the solvent polarity; in addition to the red-shift of the emission wavelength, the lifetime is changed with increasing solvent polarity (0.2 ns in hexane and 0.4 ns in THF). This behavior might be interpreted in terms of the solvation-induced electronic changes of the CT state, which would lead to a strong solvent dependence of the radiative and nonradiative processes.

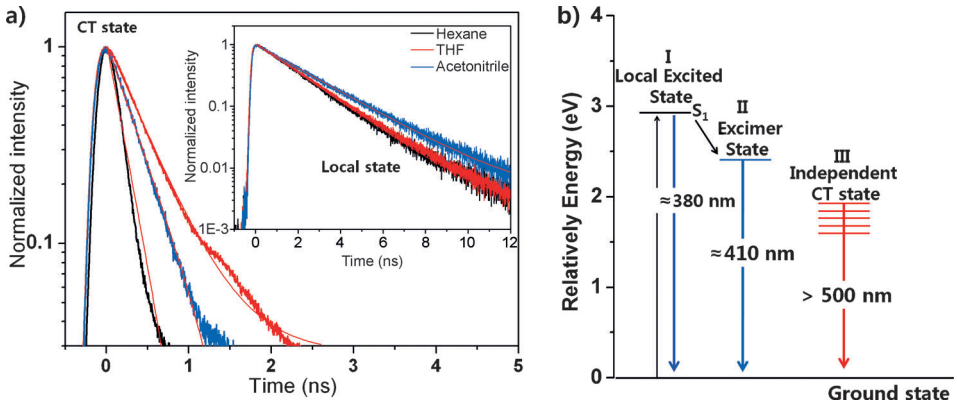

Figure 3. Emission decay profiles of **1** in various solvents monitored at a) the CT emission maxima. (Inset: at 380 nm) b) Schematic energy diagram for **1**.

To provide explicit evidence for the energy states, we performed cyclic voltammetry (CV) experiments and DFT calculations to confirm the electronic states of **1** and **2**. As shown in Figure S9, **1** and **2** exhibit reversible electrochemical behavior with two distinctive reduction waves, which corre-

spond to two sequential electron reduction processes, as confirmed by coulometry experiments (Figure S10). While the reduction waves of Ph-Cb and **2** taken at a scan rate of 100 mV s^{-1} consist of one cathodic and two anodic peaks, measurements at slower scan rates gave two separated cathodic peaks. However, reduction waves of **1** are invariant to the scan rate change; this implies the structural rigidity of **1** (Figure S11). In particular, it is worth noting that the reduction waves appear in the order of Ph-Cb (−1.96 V) < **2** (−1.75 V) < **1** (−1.32 V). As shown in Figures S12–S13, the electronic structures of **1** and **2** in the ground state were further analyzed by frontier orbital analysis. Basically, optimized geometries of **1** and **2** showed excellent agreement with X-ray single-crystal structures and all isodensity plots are mainly centered at the naphthalene units with a large HOMO–LUMO gap in the range of 4.06–5.78 eV. Compound **1**, which has a well developed CT state and a low reduction potential compared with other compounds, was selected for the electronic structure. This shows that the LUMO is largely centered at the C–C bond between the *o*-carboranyl carbon atom and the naphthyl carbon atom (C_{cage}-C_{naph}) and that the low LUMO level is well correlated with the low reduction potential. Time-dependent DFT (TD-DFT) calculations were also performed on the optimized geometries of **1** and **2**, giving simulated electronic spectra in excellent agreement with those observed in Figures S12–S13. The low-energy absorption band (> 340 nm) observed in **1** may be attributed to transitions from the highest occupied and next lower occupied orbitals (HOMO, HOMO-1) to the LUMO, and the π–π* transitions localized on the naphtyl rings or the π(naphtyl) to C-C (carborane) transitions.

On the basis of these experimental observations, the most probable mechanism of multiple emissions from the 1,2-dinaphthyl-*o*-carborane compound is shown in Figure 3b. **1** and **2** not only show local excited emission with extensive quenching and excimer emission, but also a distinctive broad CT emission at the longer wavelength exhibited. Furthermore, it is worth noting that the CT state, which is generated by the *o*-carborane cage, is isolated from the high energy of the naphthalene local excited states and the independent CT state energy level is strongly dependant on the aryl species or substituent positions, as can be seen from the comparison between **1** and **2**.

To understand the origin of the CT state and electronic perturbations induced by *o*-carborane, we focused on the C_{cage}-C_{naph} bond.[16] This is because the LUMO is largely centered on this bond and we assumed that the orbital overlap between the π-orbital of the naphthalene unit and the σ-orbital of the carbon atom of *o*-carborane is well developed through the C_{cage}-C_{naph} bond in the ground state geometry. Therefore, we attempted to change the orbital overlap by changing the torsion angle between the naphthalene plane and the carboranyl C–C bond using DFT calculations. The energetically stabilized naphthyl orientations and HOMO–LUMO isodensity plots depending on the torsion angles (10–170°) are shown in Figure 4. Based on the calculations, we indicated that the angles of energetically stabilized naphthyl orientation at lower than Δ = 0.5 eV for **1** are limited in the range of 60–100°. A rigid geometry with a perpendicular

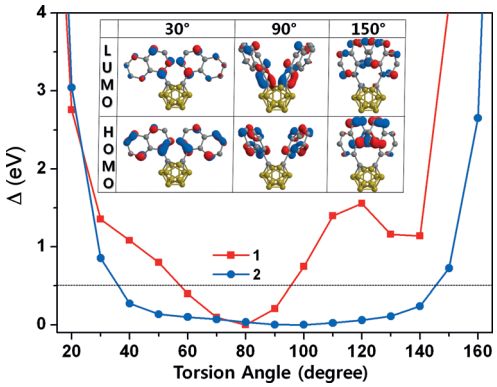

Figure 4. Theoretical calculations for energetically stabilized naphthyl orientations of **1** and **2**. (Inset: The HOMO–LUMO of **1** depending on torsion angles of 30°, 90°, and 150°.)

characteristic between the naphthalene and carboranyl C–C bonds, including the well-developed orbital overlap, is expected in both ground and excited state structures, while a less sterically restricted geometry is expected in **2** from the wide range of angles (40–140°) in stabilized naphthyl orientation (Δ < 0.5 eV). In addition, as shown in the inset of Figure 4 and in Figures S14–S15, the LUMO isodensity plots are clearly dependant on the naphthyl conformers in both **1** and **2**. This demonstrates that the perpendicular structures have large LUMO contributions at the C_{cage}-C_{naph} bond, while there is no torsion angle dependence on the HOMO and only the naphthalene-localized HOMO can be found.

These theoretical observations strongly support the well developed CT state and the lower reduction potential for **1** by rigid geometry with a perpendicular manner and stabilized LUMO by *o*-carborane. For example, different CT emission quantum yields (QY) depending on the 1- and 2-naphthalene substitution are explained by the rigidity of the naphthyl geometry with a degree of orbital overlap; this shows a higher CT emission with lower local emission QYs in **1**. Moreover, the low reduction potential with distinctive two reduction waves and elongated *o*-carboranyl C-C distance of **1** are also possibly explained by the well-developed orbital overlap between the naphthalene and carboranyl C–C bonds.

To confirm our speculation, as shown in Figure S5, we measured the low temperature (at 77 K) in 2-methyltetrahydrofuran (2-MeTHF) solution and the neat film PL spectra for fixation of naphthyl conformers and observed enhanced CT emissions in both **1** and **2**, while there was no emission in Ph-Cb. In addition, almost similar CT emissions are shown between the 2-MeTHF solution (536 nm for **1**, 506 nm for **2**) and the neat film (530 nm for **1**, 500 nm for **2**). From these results, we assumed that there are no intermolecular interactions in aggregated states and emission originates only from the intramolecular charge transfer (ICT) state,[6a,17] that is, from the intramolecular through-bond interactions between the naphthalene unit and *o*-carborane cage. Furthermore, the different maximum ICT emissions between **1** and **2** are well correlated with the reduction potentials observed in the CV experiments, showing a lower reduction potential of **1**. As a result, we suggest that the multiple photoluminescence in *o*-

carborane originates from the orbital overlap between the naphthyl π-orbital and the carboranyl σ(C-C) orbital allowing the formation of a new type of ICT state.

Experimental Section

Synthesis: 1,2-Bis(1-naphthyl)-*ortho*-carborane (**1**) and 1,2-bis(2-naphthyl)-*ortho*-carborane (**2**) were synthesized from 1- or 2-bromonaphtalene by reaction of 1,2-di(naphthalen)ethyne with decaborane in two steps, as shown in Scheme S1. All products were isolated using flash column chromatography and further purified using train sublimation in a moderate yield. Full experimental details can be found in the Supporting Information.

Received: May 20, 2013
Published online: July 23, 2013

Keywords: carborane cages · charge transfer · excited states · multiple photoluminescence · photochemistry

[1] a) W. Rettig, *Angew. Chem.* **1986**, *98*, 969; *Angew. Chem. Int. Ed. Engl.* **1986**, *25*, 971; b) K. Becker, J. M. Lupton, *J. Am. Chem. Soc.* **2005**, *127*, 7306; c) W. Lin, L. Yuan, Z. Cao, Y. Feng, J. Song, *Angew. Chem.* **2010**, *122*, 385; *Angew. Chem. Int. Ed.* **2010**, *49*, 375; d) C. Li, Y. Zhang, J. Hu, J. Cheng, S. Liu, *Angew. Chem.* **2010**, *122*, 5246; *Angew. Chem. Int. Ed.* **2010**, *49*, 5120.

[2] N. J. Turro, *Modern molecular photochemistry*, 1st ed., University Science Books, Sausalito, **1991**.

[3] a) D. F. Duxbury, *Chem. Rev.* **1993**, *93*, 381; b) K. E. Sapsford, L. Berti, I. L. Medintz, *Angew. Chem.* **2006**, *118*, 4676; *Angew. Chem. Int. Ed.* **2006**, *45*, 4562.

[4] C.-C. Hsieh, C.-M. Jiang, P.-T. Chou, *Acc. Chem. Res.* **2010**, *43*, 1364.

[5] H. Saigusa, E. C. Lim, *Acc. Chem. Res.* **1996**, *29*, 171.

[6] a) Z. R. Grabowski, K. Rotkiewicz, W. Rettig, *Chem. Rev.* **2003**, *103*, 3899; b) R. R. Hu, E. Lager, A. Aguilar-Aguilar, J. Z. Liu, J. W. Y. Lam, H. H. Y. Sung, I. D. Williams, Y. C. Zhong, K. S. Wong, E. Pena-Cabrera, *J. Phys. Chem. C* **2009**, *113*, 15845; c) Y. Qian, M. M. Cai, L. H. Xie, G. Q. Yang, S. K. Wu, W. Huang, *ChemPhysChem* **2011**, *12*, 397.

[7] a) N. Nakashima, M. Murakawa, N. Mataga, *Bull. Chem. Soc. Jpn.* **1976**, *49*, 854; b) W. Rettig, W. Majenz, *J. Photochem. Photobiol. A* **1992**, *65*, 95.

[8] a) K.-R. Wee, W.-S. Han, D. W. Cho, S. Kwon, C. Pac, S. O. Kang, *Angew. Chem.* **2012**, *124*, 2731; *Angew. Chem. Int. Ed.* **2012**, *51*, 2677; b) K.-R. Wee, Y.-J. Cho, S. Jeong, S. Kwon, J.-D. Lee, I.-H. Suh, S. O. Kang, *J. Am. Chem. Soc.* **2012**, *134*, 17982.

[9] a) J. J. Peterson, M. Werre, Y. C. Simon, E. B. Coughlin, K. R. Carter, *Macromolecules* **2009**, *42*, 8594; b) B. P. Dash, R. Satapathy, E. R. Gaillard, J. A. Maguire, N. S. Hosmane, *J. Am. Chem. Soc.* **2010**, *132*, 6578; c) J. J. Peterson, A. R. Davis, M. Werre, E. B. Coughlin, K. R. Carter, *ACS Appl. Mater. Interfaces* **2011**, *3*, 1796; d) A. R. Davis, J. J. Peterson, K. R. Carter, *ACS Macro Lett.* **2012**, *1*, 469.

[10] a) *Handbook of Fluorescence Spectra of Aromatic Molecules* (Ed.: I. B. Berlman), Academic Press, New York, **1971**; b) R. Tsuji, K. Komatsu, Y. Inoue, K. Takeuchi, *J. Org. Chem.* **1992**, *57*, 636.

[11] a) R. N. Grimes, *Carboranes*, 2nd ed.; Acadamic Press, **2011**; b) V. I. Bregadze, *Chem. Rev.* **1992**, *92*, 209; c) J. Ko, S. O. Kang, *Adv. Organomet. Chem.* **2001**, *47*, 61.

[12] a) E. S. Alekseyeva, M. A. Fox, J. A. K. Howard, J. A. H. MacBride, K. Wade, *Appl. Organomet. Chem.* **2003**, *17*, 499; b) K. Ohta, T. Goto, Y. Endo, *Inorg. Chem.* **2005**, *44*, 8569; c) E. Hao, B. Fabre, F. R. Fronczek, M. G. H. Vicente, *Chem. Commun.* **2007**, 4387; d) K. Kokado, Y. Chujo, *J. Org. Chem.* **2011**, *76*, 316.

[13] a) M. G. Davidson, T. G. Hibbert, J. A. K. Howard, A. Mackinnon, K. Wade, *Chem. Commun.* **1996**, 2285; b) M. A. Fox, C. Nervi, A. Crivello, P. J. Low, *Chem. Commun.* **2007**, 2372; c) J. M. Oliva, N. L. Allan, P. v. R. Schleyer, C. Vinas, F. Teixidor, *J. Am. Chem. Soc.* **2005**, *127*, 13538; d) B. W. Hutton, F. MacIntosh, D. Ellis, F. Herisse, S. A. Macgregor, D. McKay, V. P. Armstrong, G. M. Rosair, D. S. Perekalin, H. Tricas, A. J. Welch, *Chem. Commun.* **2008**, 5345.

[14] a) S. R. Patil, S. B. Patwari, *J. Lumin.* **1999**, *82*, 115; b) C. Reylé, P. Brechignac, *Eur. Phys. J. D* **2000**, *8*, 205; c) H. Maeda, T. Maeda, K. Mizuno, *Molecules* **2012**, *17*, 5108.

[15] a) A. A. Kazzaz, I. H. Munro, *Proc. Phys. Soc.* **1966**, *87*, 329; b) K. Uchida, M. Tanaka, M. Tomura, *J. Lumin.* **1979**, *20*, 409.

[16] a) L. A. Boyd, W. Clegg, R. C. B. Copley, M. G. Davidson, M. A. Fox, T. G. Hibbert, J. A. K. Howard, A. Mackinnon, R. J. Peacea, K. Wade, *Dalton Trans.* **2004**, 2786; b) L. Weber, J. Kahlert, R. Brockhinke, L. Bçhling, A. Brockhinke, H.-G. Stammler, B. Neumann, R. A. Harder, M. A. Fox, *Chem. Eur. J.* **2012**, *18*, 8347; c) L. Weber, J. Kahlert, L. Böhling, A. Brockhinke, H.-G. Stammler, B. Neumann, R. A. Harder, P. J. Low, M. A. Fox, *Dalton Trans.* **2013**, *42*, 2266.

[17] M. Volkhard, K. Oliver, *Charge and Energy Transfer Dynamics in Molecular Systems*, Wiley-VCH, Weinheim, **2004**.

